



Patterning method for silicides based on local oxidation

S. Mantl, M. Dolle, St. Mesters, P. F. P. Fichtner, and H. L. Bay

Citation: *Applied Physics Letters* **67**, 3459 (1995); doi: 10.1063/1.115246

View online: <http://dx.doi.org/10.1063/1.115246>

View Table of Contents: <http://scitation.aip.org/content/aip/journal/apl/67/23?ver=pdfcov>

Published by the [AIP Publishing](#)

Articles you may be interested in

[Localized conductive patterning via focused electron beam reduction of graphene oxide](#)

Appl. Phys. Lett. **106**, 133109 (2015); 10.1063/1.4917038

[An investigation of acoustic beam patterns for the sonar localization problem using a beam based method](#)

J. Acoust. Soc. Am. **133**, 4044 (2013); 10.1121/1.4802831

[An x-ray spectromicroscopic study of the local structure of patterned titanium silicide](#)

Appl. Phys. Lett. **71**, 55 (1997); 10.1063/1.119467

[Localization of sources by two pattern-match methods](#)

J. Acoust. Soc. Am. **87**, S35 (1990); 10.1121/1.2028184

[Anodic oxidation of tantalum silicide](#)

Appl. Phys. Lett. **47**, 579 (1985); 10.1063/1.96077

The image shows the cover of an Applied Physics Reviews journal. It features a 3D diagram of a layered structure with various components labeled. The text 'AIP Applied Physics Reviews' is at the top left. The background is a blue gradient with a bright light source on the right and a molecular structure of blue spheres on the left.

NEW Special Topic Sections

NOW ONLINE
Lithium Niobate Properties and Applications:
Reviews of Emerging Trends

AIP Applied Physics Reviews

Patterning method for silicides based on local oxidation

S. Mantl,^{a)} M. Dolle, St. Mesters, P. F. P. Fichtner,^{b)} and H. L. Bay
Institut für Schicht- und Ionentechnik, KFA Jülich, D-52425 Jülich, Germany

(Received 13 June 1995; accepted for publication 26 September 1995)

Oxidation of CoSi_2 layers on $\text{Si}(100)$ using oxidation masks has been investigated. It is shown that local oxidation can be used to pattern the silicide layer. This method allows the formation of buried interconnects and metallized silicon mesa structures. Epitaxial CoSi_2 silicide layers were grown by molecular beam epitaxy on $\text{Si}(100)$. The $\text{SiO}_2/\text{Si}_3\text{N}_4$ oxidation mask was patterned photolithographically with linewidths of typically $1.5 \mu\text{m}$. During thermal oxidation, SiO_2 forms in the unprotected regions of the silicide layer. The silicide is pushed into the substrate in these regions. At a critical oxide thickness, the oxidized region of the silicide layer separates from the unoxidized, in conformance with the structure of the oxidation mask. The oxide capped silicide maintains its uniform layer structure and its single crystallinity in spite of the large shift into the substrate. The method should be applicable also to polycrystalline silicides, such as TiSi_2 . © 1995 American Institute of Physics.

Transition metal silicides are the materials of choice for contacts and interconnects in microelectronic devices or as Schottky contacts in infrared detectors.¹ Some silicides, e.g., CoSi_2 , NiSi_2 , can be grown epitaxially and thus integrated in silicon based epitaxial silicon/metal/silicon heterostructures.² Such structures are highly useful for new electronic and electro-optic devices, in particular for the realization of new vertical devices.^{3,4} The stability of silicides against oxidation is essential for device processing and has been studied in detail.⁵⁻⁷ Most transition metal silicides form a silicon dioxide layer on top of the silicide layer during oxidation. The oxidation process of transition metal silicides consists basically of four major steps:⁶ (1) diffusion of the oxidant through the SiO_2 layer; (2) dissociation of the silicide at the SiO_2 -silicide interface; (3) transport of the metal or the silicon through the silicide layer; (4) silicide formation at the silicide-silicon interface. In the case of CoSi_2 , Co diffuses through the silicide layer and forms again the disilicide phase at the silicide-substrate interface. The dissociation of the silicide at the upper interface and its reformation at the lower interface yield to an apparent inertness of the silicide layer against oxidation. For device application it is important that the silicide layer preserves its integrity. Interestingly, the SiO_2 layer on top of the silicide has properties close to thermally grown SiO_2 on Si, i.e., the dielectric constants and the density of the oxide are similar to those of SiO_2 thermally grown on Si.⁶ However, the dielectric strength is lower, most probably due to the roughness of the oxide/silicide interface. The thickness of the SiO_2 layer is fairly constant even on top of a rather rough silicide layer, as revealed by transmission electron microscopy⁷ (TEM). We expect an improvement of the dielectric strength of SiO_2 on highly uniform epitaxial CoSi_2 layers.

In this letter we present investigations of uniform and

local oxidation of epitaxial CoSi_2 layers on $\text{Si}(100)$. We will show for the first time, that local oxidation of a silicide layer can be used to pattern the silicide layer and form metallized mesa-structures, simply by the use of an appropriate mask during thermal oxidation. The development of the method was guided by the well established technology of local oxidation of silicon (LOCOS), which is broadly used for lateral isolation of ULSI devices.⁸ In addition, we will show that epitaxial silicide layers preserve their single crystalline quality during oxidation.

First, we will discuss the oxidation of uniform epitaxial CoSi_2 surface layers on $\text{Si}(100)$. The silicide was grown by molecular beam epitaxy at 525°C followed by a high temperature anneal as described elsewhere.⁹ Subsequently, rapid thermal annealing (RTA) was performed at 1150°C for 30 s in order to form a uniform silicide layer. Such CoSi_2 layers are single crystalline and have a very low specific electrical resistivity of $14 \mu\Omega \text{ cm}$ at room temperature. Figure 1 shows Rutherford backscattering spectrometry (RBS) spectra of

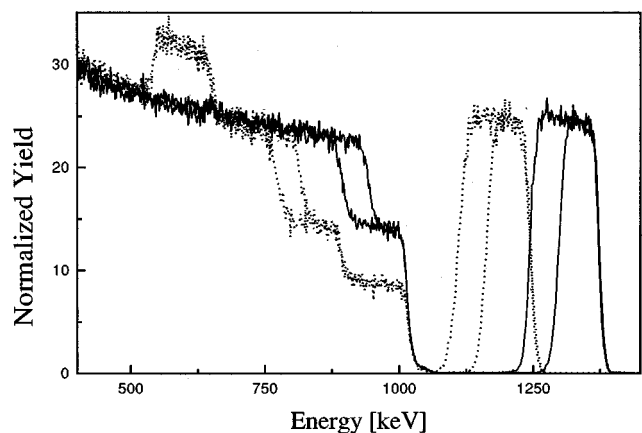


FIG. 1. Rutherford backscattering spectra of epitaxial CoSi_2 layers on $\text{Si}(100)$ with thicknesses of 90 and 150 nm, before (solid line) and after wet oxidation (dotted line) at 980°C for 20 min. The spectra were measured with 1.8 MeV He^+ ions at a tilt angle of 7° and a scattering angle of 170° .

^{a)}Electronic mail: s.mantl@kfa-juelich.de

^{b)}Permanent address: Department of Metallurgy, UFRGS, AV. Bento Gonçalves, 9500-Caixa Postal 15051, 91501-970 Porto Alegre, RS, Brasilien.

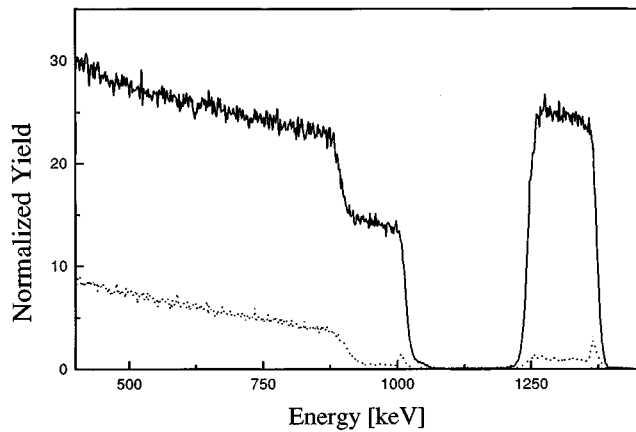


FIG. 2. Random and (001) aligned RBS spectra of a 150 nm CoSi₂ layer on Si(100) after wet oxidation at 980 °C for 20 min. The channeling spectrum (dotted line) shows a minimum yield of the silicide of 4%, indicating an excellent single crystalline quality. The SiO₂ layer was removed wet chemically before the RBS measurements.

two silicide layers with different thicknesses, 90 nm and 150 nm, before and after wet oxidation. After wet oxidation at 980 °C for 20 min the CoSi₂ layers preserved their structural properties, although they were shifted into the substrate by about 150 nm. The RBS data show a large shift of the Co signals but no changes of the Co signal shape. This is an important point, because it demonstrates the chemical and structural stability of the layer during the oxidation process. Interestingly, the O signals of the two samples overlap perfectly indicating identical thicknesses of the SiO₂ layers of ≈ 250 nm. Therefore, the oxidation rate is independent of the silicide thickness, in agreement with previous investigations showing that the diffusive transport through the silicide is not the rate limiting step.⁶ Furthermore, the single crystallinity of the oxidized silicide layer remains unchanged as compared to the virgin sample. The minimum channeling yield (Fig. 2) of the oxidized silicide layer of 4% is the same as that of the virgin sample (not shown), indicating the excellent quality of the single crystalline layer.

The oxidation rates of the single crystalline CoSi₂ layers were measured by Rutherford backscattering during dry oxidation and wet oxidation (not shown). Generally, we found that for both dry and wet oxidation the surface layer of SiO₂ grows parabolically with time. In order to reduce the thermal budget we used wet oxidation at 980 °C for the local oxidation experiment. At that temperature we measured the parabolic oxidation rate constant $B=50 \text{ nm}^2 \text{ s}^{-1}$. The oxidation rates of the silicide is significantly larger than for pure silicon, in agreement with previous work.⁶

The basic steps of the local oxidation of a silicide (LOCOSI) process are sketched in Fig. 3. An oxidation mask consisting of a 20 nm thin, thermally grown SiO₂ layer and a CVD Si₃N₄ layer with a typical thickness of 200 nm was deposited. Oxidation leads to growth of SiO₂ in the openings of the oxidation mask, the silicide layer is pushed deeper into the substrate, and thus deformed at the transition between the oxidized and protected regions. The silicide layer undulates but remains continuous. At a critical oxide thickness, depending on the thickness of the silicide, the layer disrupts

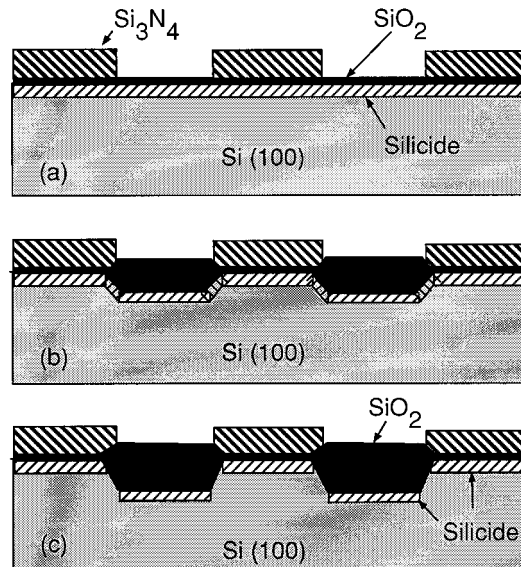


FIG. 3. Illustration of the local process of oxidation of silicides (LOCOSI) allowing lateral patterning of silicide layers. (a) The silicide layer is covered with a thin SiO₂ layer and a patterned Si₃N₄ layer. (b) Oxidation yields to growth of SiO₂ locally. The silicide layer undulates but remains continuous. (c) At a critical oxide thickness, the silicide layer breaks up and forms a pattern conform with the oxidation mask. This process produces buried interconnects and/or metallized silicon-mesa structures.

exactly below the edges of the oxidation mask. This is shown in a cross-sectional transmission electron microscopy (XTEM) micrograph (Fig. 4) of a sample wet oxidized at 980 °C for 45 min. The oxidized silicide line is perfectly separated from the silicide surface layer due to its shift into the substrate by about 150 nm. As visible in Figs. 3 and 4, metallized silicon mesa structures were obtained, where the two silicide layers are connected electrically only via the silicon substrate. The buried silicide line is passivated by the thermally grown oxide. Before oxidation the thickness of the silicide layer amounted ≈ 55 nm. In the oxidized region it decreased in average to ≈ 50 nm whereas in the unoxidized region it increased up to ≈ 80 nm near the edges (Fig. 4). Interestingly, despite the large material redistribution along the silicide layer, the uniformity of the individual layers is remarkably good. Furthermore, we observed that longer oxidation or additional annealing reduce the variation in thickness. The dark contrasts under the silicide layer in the XTEM image show strain contrasts. In spite of the presence of stress, introduced by the local oxidation process and the lat-

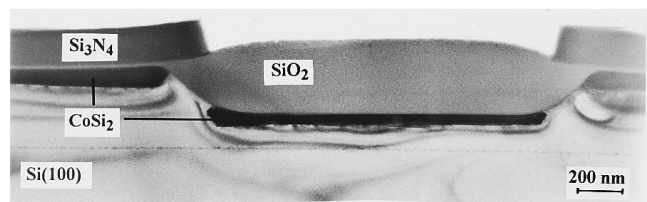


FIG. 4. Cross-sectional TEM micrograph of a 55 nm thick CoSi₂ layer patterned by local oxidation. The linewidth of the oxidation mask is 1.5 μm. The thickness of the upper silicide layer amounts 60–80 nm and that of the buried ≈ 50 nm after oxidation.

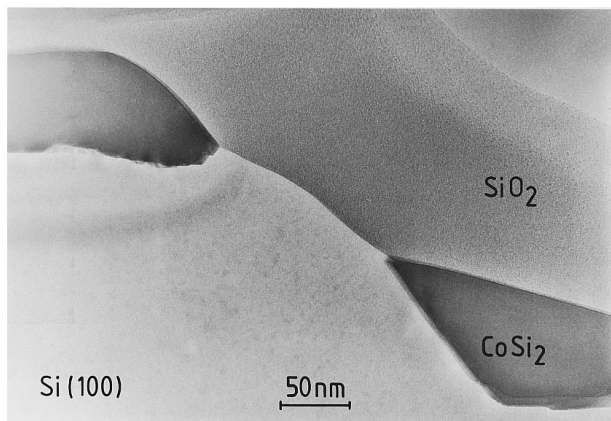


FIG. 5. XTEM micrograph of the transition region of the sample of Fig. 4 showing a smooth SiO_2 /silicon substrate interface between the two upper and lower silicide layers. No dislocations are observed.

tice mismatch of the single crystalline CoSi_2 layer of -1.2% , no dislocations in the silicon were observed. This is verified by the XTEM image of Fig. 5, showing the transition region in an enlarged scale. The appearance of dislocations at these regions has been reported for silicon locally oxidized with non optimized thicknesses of the oxidation masks.⁸ The SiO_2 /silicon interface is strikingly smooth, and in particular, no traces of silicide precipitates are seen. These observations are most important for microelectronic or optoelectronic applications.

The key question of the new patterning method refers to the driving force for the break up of the silicide layer. At present, we assume that the disruption of the silicide in conformance with the nitride mask is related to the stress field introduced by the local growth of the SiO_2 layer and the lattice mismatch between the silicide and the silicon substrate. Stress calculations of locally oxidized silicon showed large stresses, localized at the edges.¹⁰ We believe that the stress field generates a chemical potential gradient in the transition regions in such a way that after dissociation of the

silicide at the SiO_2 -silicide interface the Co diffuses no longer primarily along the shortest path through the silicide layer, as it is the case in the planar regions, but preferentially toward the upper and lower silicide layers. Such an effectively anisotropic diffusion flux of Co atoms causes first thinning of the silicide layer and second, break up at the high stress points. This phenomenon will be investigated further.

In summary, we have demonstrated that local oxidation can be used to pattern silicide layers. The oxidized silicide layer is buried under a passivating silicon dioxide layer. The new method allows the formation of buried, passivated interconnects and metallized silicon mesa-structures. In view of the lack of dry etching processes for CoSi_2 , there exist no appropriate Co-chloride or -fluoride gases, this patterning method may become highly useful. Technologically, it would be highly desirable to apply this process on polycrystalline silicide layers. First local oxidation experiments on polycrystalline TiSi_2 layers look promising. However, because of the grain structure and the larger interface roughness, the polycrystalline layers are less temperature stable than the single crystalline layers, and thus the process conditions become more critical, in order to avoid layer disintegration.

¹R. W. Fathauer, S. Mantl, L. J. Schowalter, and K. N. Tu, eds., Mater. Res. Soc. Symp. Proc. **320** (1994).

²L. J. Chen and K. N. Tu, Mater. Sci. Rep. **6**, 53 (1991); R. T. Tung, Mater. Chem. Phys. **32**, 107 (1992); H. v. Känel, Mater. Sci. Rep. **8**, 193 (1992).

³A Schüppen, L. Vescan, M. Marso, A. v. d. Hart, H. Lüth, and H. Beneking, Electron. Lett. **29**, 215 (1993).

⁴J. P. Hermanns, F. Rüdgers, E. Stein von Kamienski, H. G. Roskos, H. Kurz, O. Hollricher, C. Buchal, and S. Mantl, Appl. Phys. Lett. **66**, 866 (1995).

⁵W. J. Strydom, J. C. Lombaard, and R. Pretorius, Thin Solid Films **131**, 215 (1985).

⁶H. Jiang, C. S. Petersson, and M.-A. Nicolet, Thin Solid Films **140**, 115 (1986).

⁷G. J. Huang and L. J. Chen, J. Appl. Phys. **76**, 865 (1994).

⁸S. Wolf, Solid State Technol. **35**, 53 (1992).

⁹S. Mantl and H. L. Bay, Appl. Phys. Lett. **61**, 267 (1992).

¹⁰I. De Wolf, J. Vanhellefont, A. Romano-Rodriguez, H. Norström, and H. E. Maes, J. Appl. Phys. **71**, 898 (1992).